

- (1973); J. D. Corbett, *Inorg. Chem.*, **7**, 198 (1968).
- (3) See, for example, C. F. Dykstra, H. F. Schaefer, and W. Meyer, *J. Chem. Phys.*, **65**, 5141 (1976).
- (4) E. L. Muetterties, *Bull. Soc. Chim. Belg.*, **84**, 959 (1975).
- (5) K. H. Johnson and R. P. Messmer, *J. Vac. Sci. Technol.*, **11**, 236 (1974).
- (6) D. W. Turner, C. Baker, A. D. Baker, and C. R. Brundle, "Molecular Photoelectron Spectroscopy", Wiley-Interscience, New York, N.Y., 1970; T. J. Koopmans, *Physica*, **1**, 104 (1934).
- (7) H. Bock and B. G. Ramsey, *Angew. Chem., Int. Ed. Engl.*, **12**, 734 (1973).
- (8) E. L. Muetterties, "Boron Hydride Chemistry", Academic Press, New York, N.Y., 1975.
- (9) W. N. Lipscomb, "Boron Hydrides", W. A. Benjamin, New York, N.Y., 1963; R. E. Williams, *Inorg. Chem.*, **10**, 210 (1971).
- (10) Evidence has been presented for a fourth structural class. See M. Mangion, R. K. Hertz, M. L. Denniston, J. R. Long, W. R. Clayton, and S. G. Shore, *J. Am. Chem. Soc.*, **98**, 449 (1976).
- (11) K. Wade, *J. Chem. Soc., Chem. Commun.*, 792 (1972); *Inorg. Nucl. Chem. Lett.*, **8**, 559 (1972).
- (12) K. Wade, *Adv. Inorg. Chem. Radiochem.*, **18**, 1 (1976); R. E. Williams, *ibid.*, **18**, 67 (1976); R. W. Rudolph, *Acc. Chem. Res.*, **9**, 446 (1976).
- (13) W. N. Lipscomb in "Boron Hydride Chemistry", E. L. Muetterties, Ed., Academic Press, New York, N.Y., 1975, p 39.
- (14) Note that the valence bond approach is not directly useful in the consideration of photoelectron spectra.
- (15) T. P. Fehlner, *Inorg. Chem.*, **14**, 934 (1975).
- (16) J. A. Ulman and T. P. Fehlner, *J. Am. Chem. Soc.*, **98**, 1119 (1976).
- (17) D. R. Lloyd, N. Lynaugh, P. J. Roberts, and M. F. Guest, *J. Chem. Soc., Faraday Trans. 2*, 1382 (1975).
- (18) See, for example, W. Ensslin, H. Bock, and G. Beker, *J. Am. Chem. Soc.*, **96**, 2757 (1974).
- (19) See, for example, F. O. Ellison, *J. Am. Chem. Soc.*, **85**, 3540 (1963); J. C. Tully, *J. Chem. Phys.*, **64**, 3182 (1976).
- (20) J. W. Rabalais, "Principles of Ultraviolet Photoelectron Spectroscopy", Wiley, New York, N.Y., 1977, p 283.
- (21) R. Hoffmann and W. N. Lipscomb, *J. Chem. Phys.*, **36**, 2179 (1962).
- (22) This restriction will be relaxed in the following paper.
- (23) See ref 8 for structures.
- (24) Professor S. G. Shore, Ohio State University.
- (25) J. A. Ulman, Ph.D. Thesis, University of Wisconsin, 1974.
- (26) Chemical Systems Inc., Irvine, Calif.
- (27) Callery Chemical Co., Callery, Pa.
- (28) H. D. Johnson, II, V. T. Brice, and S. G. Shore, *Inorg. Chem.*, **12**, 689 (1973).
- (29) T. Onak, R. P. Drake, and G. B. Dunks, *Inorg. Chem.*, **3**, 1686 (1964).
- (30) R. E. Ballard, *Appl. Spectrosc. Rev.*, **7**, 183 (1973).
- (31) See, for example, P. Dechant, A. Schweig, and W. Thiel, *Angew. Chem., Int. Ed. Engl.*, **12**, 308 (1973).
- (32) I. R. Epstein, T. F. Koetzle, R. M. Stevens, and W. N. Lipscomb, *J. Am. Chem. Soc.*, **92**, 7019 (1970).
- (33) This designation has been used by others: T. C. Waddington, *Trans. Faraday Soc.*, **63**, 1313 (1967); D. M. P. Mingos, *J. Chem. Soc., Dalton Trans.*, 20 (1977).
- (34) F. A. Cotton, "Chemical Applications of Group Theory", Wiley, New York, N.Y., 1971.
- (35) D. S. Marynick and W. N. Lipscomb, *J. Am. Chem. Soc.*, **94**, 8692 (1972).
- (36) R. W. Jones and W. S. Koski, *J. Chem. Phys.*, **59**, 1228 (1973).
- (37) E. Switkes, I. R. Epstein, J. A. Tossell, R. M. Stevens, and W. N. Lipscomb, *J. Am. Chem. Soc.*, **92**, 3837 (1970).
- (38) T. P. Fehlner and D. W. Turner, *J. Am. Chem. Soc.*, **95**, 7175 (1973).
- (39) M. Okuda and N. Jonathan, *J. Electron Spectrosc. Relat. Phenom.*, **3**, 19 (1974).
- (40) C. R. Brundle, M. B. Robin, H. Basch, M. Pinsky, and A. Bond, *J. Am. Chem. Soc.*, **92**, 3863 (1970).
- (41) I. R. Epstein, J. A. Tossell, E. Switkes, R. M. Stevens, and W. N. Lipscomb, *Inorg. Chem.*, **10**, 171 (1971).
- (42) D. S. Marynick and W. N. Lipscomb, *J. Am. Chem. Soc.*, **94**, 8699 (1972).
- (43) G. Beltram and T. P. Fehlner, in preparation.
- (44) Note Added in Proof: Calculations on 1,5-C₂B₃H₅ have appeared in: N. J. Fitzpatrick and M. O. Fanning, *J. Mol. Struct.*, **40**, 271 (1977), and M. F. Guest and I. H. Hillier, *Mol. Phys.*, **26**, 435 (1973).

Characterization of Ferraboranes by Ultraviolet Photoelectron Spectroscopy

J. A. Ulman, E. L. Andersen, and T. P. Fehlner*

Contribution from the Department of Chemistry, University of Notre Dame, Notre Dame, Indiana 46556. Received June 6, 1977

Abstract: The He(I) and Ne(I) photoelectron spectra of C₂B₃H₅Fe(CO)₃, C₂B₃H₇Fe(CO)₃, B₄H₈Fe(CO)₃, B₅H₉Fe(CO)₃, and B₅H₃Fe(CO)₅ are reported. Spectra are assigned utilizing observed band characteristics and an empirical model based on an analysis of the spectra of boranes and carboranes of similar size and structure. Comparison of B₄H₈Fe(CO)₃ with B₅H₉ and C₄H₄Fe(CO)₃ reveals that the electronic structure of the borane is a good model for the ferraborane. Characteristic features of the spectra of B₅H₉Fe(CO)₃ suggest a close relationship to B₆H₁₀ while observations on B₅H₃Fe(CO)₅ are consistent with a structure involving 2CO molecules bound to the cage in exo-polyhedral positions. The nature of the perturbation of the iron atom by the cage and the cage by the iron atom is also revealed in the analysis of the spectra.

Recently a number of compounds containing a borane framework and one iron tricarbonyl group have been discovered and characterized.¹⁻³ These ferraboranes and related ferracarboranes have small enough structures and sufficient volatility such that they can be conveniently investigated with the technique of valence level photoelectron spectroscopy. As the photoelectron spectrum is directly related to the electronic structure of the molecule cast in a one-electron molecular orbital description,⁴ this technique provides a means of probing the nature of the metal-cage interaction. The usual means of analyzing photoelectron spectra involves the utilization of quantum chemical calculations. With metals this presents some difficulties. First, quantitative calculations involving metals require more than a casual, semiempirical approach, and, second, comparison of good calculated energy levels with photoelectron spectra has provided evidence for exceedingly large Koopmans' defects for orbitals having large metal d character.⁵ In the preceding paper⁶ in which the electronic

structure of small pyramidal and bipyramidal boranes and carboranes was considered, we presented an alternative to calculations. In this approach the photoelectron spectra of model compounds are used as sources of parameters for a qualitative description of related compounds. This method is adopted here to describe the spectra of ferracarboranes and ferraboranes and also to reveal the behavior of an iron atom in the environment generated by the borane cage.

The interaction of transition metals with borane and carborane cages has been and still is of great interest.⁷ In terms of a valence bond description, there are at least three distinct ways known by which a metal is coupled to a cage. In one a single atom of the cage is bonded to the metal by a two-electron, two-center bond and the metal functions as any other exo-polyhedral ligand. In the second the metal is in a bridging position of the cage and the interaction is considered to take place through a three-center, two-electron bond. In the third, the metal may be considered as interacting with the cage by

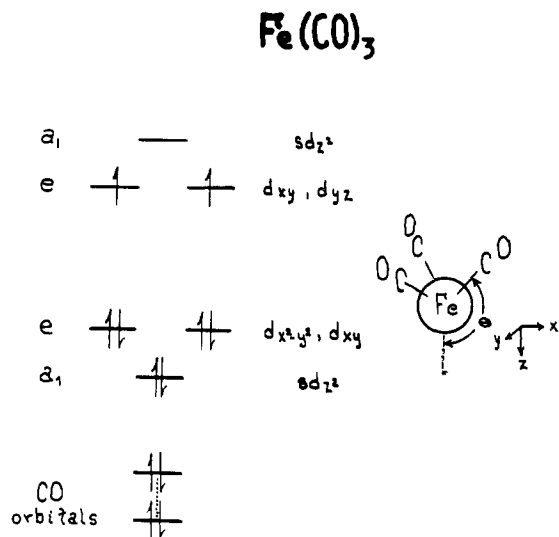


Figure 1. A schematic diagram of the orbital structure of the $\text{Fe}(\text{CO})_3$ fragment for an angle θ of 130° according to ref 13.

means of one or more multicenter, two-electron interactions. It is the last situation that is the focus of this work.

In the last case, there are two popular views of how the metal interacts with the cage. In the organometallic view the cage acts as a polyhapto ligand which formally contributes electrons to the metal such that the 18-electron rule is satisfied. Historically, this view of the cage-metal interaction served as the basic rationale for the first successful approach to the synthesis of metal-containing cages.⁸

The second view of metals bound to cages envisions the metal as being simply another atomic member of a cage or atom cluster containing both metal and nonmetal atoms. In this approach a distinction is made between cluster or framework bonding (endo-polyhedral bonding) and the bonds to atoms outside of the cluster (exo-polyhedral bonding). As part of the cage, the metal contributes three orbitals and a number of electrons that depends on the metal and the exo-polyhedral substituents on the metal. Simple electron counting rules have been established so that the geometrical arrangement of the cluster atoms can be predicted.⁹ From this viewpoint the structures of metal-containing cages and organometallic compounds are derived from borane models. Recent approximate calculations have further explored this idea.¹⁰

The two views of how metals interact with cages merge in the molecule $\text{B}_4\text{H}_8\text{Fe}(\text{CO})_3$. This compound can be viewed as either a derivative of the borane B_5H_9 or as a close relative of the structurally similar organometallic compound, $\text{C}_4\text{H}_4\text{Fe}(\text{CO})_3$. Thus, the work presented below provides an experimental comparison of these views.

Experimental Section

The photoelectron spectra of $\text{C}_2\text{B}_3\text{H}_5\text{Fe}(\text{CO})_3$, $\text{C}_2\text{B}_3\text{H}_7\text{Fe}(\text{CO})_3$, $\text{B}_4\text{H}_8\text{Fe}(\text{CO})_3$, $\text{C}_4\text{H}_4\text{Fe}(\text{CO})_3$, $\text{B}_5\text{H}_9\text{Fe}(\text{CO})_3$, and $\text{B}_5\text{H}_3\text{Fe}(\text{CO})_5$ were recorded in the gaseous state using the He(I) (21.2 eV) and Ne(I) (16.8 eV) lines at a resolution of 25 meV (fwhm) at 5 eV electron energy. The spectrometer was calibrated using a mixture of xenon and argon as an internal standard. Samples were run at room temperature.

The $\text{C}_4\text{H}_4\text{Fe}(\text{CO})_3$ was purchased from Strem Chemicals, Danvers, Mass., and was purified by vacuum line fractionation before use. The ferraboranes and ferracarboranes were prepared and purified as reported in the literature: $\text{C}_2\text{B}_3\text{H}_5\text{Fe}(\text{CO})_3$,¹¹ $\text{C}_2\text{B}_3\text{H}_7\text{Fe}(\text{CO})_3$,¹² $\text{B}_4\text{H}_8\text{Fe}(\text{CO})_3$,¹ $\text{B}_5\text{H}_9\text{Fe}(\text{CO})_3$,² and $\text{B}_5\text{H}_3\text{Fe}(\text{CO})_5$.³ Purity of samples was checked by either mass spectrometric analysis or ^{11}B NMR spectroscopy.

The $\text{Fe}(\text{CO})_3$ Fragment. In the preceding paper⁶ an empirical model, the ring-polar model, was developed to treat the photoelectron spectra

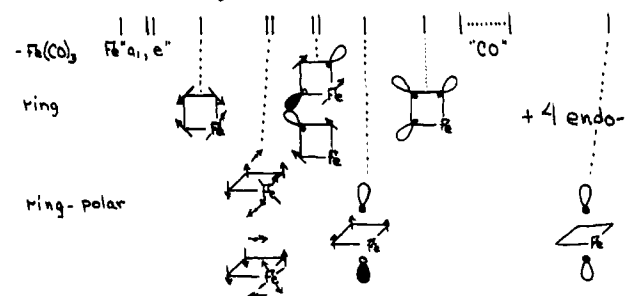
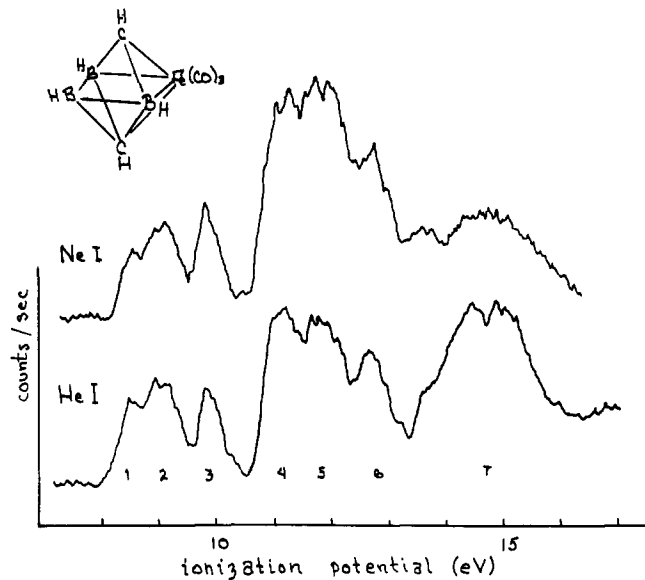


Figure 2. The photoelectron spectra of $\text{C}_2\text{B}_3\text{H}_5\text{Fe}(\text{CO})_3$ and the orbital assignments of the observed bands.

of small cages. In this model the molecular orbitals of the system were partitioned into two types: transferable orbitals associated with the ring and polar fragments and orbitals associated with the ring-polar interactions. Empirical parameters were developed for three-, four-, and five-membered rings and the BH and CH polar fragments. Thus, in order to apply this model to ferraboranes, it is only necessary to develop parameters for the $\text{Fe}(\text{CO})_3$ fragment.

The $\text{Fe}(\text{CO})_3$ fragment has been investigated theoretically and the orbital structure of this fragment is represented in Figure 1.¹³ In terms of bonding capabilities, the $\text{Fe}(\text{CO})_3$ fragment is much like BH; however, in terms of photoelectron spectroscopy there will be a number of visible differences. Replacing BH by $\text{Fe}(\text{CO})_3$ will result in the loss of one band corresponding to the ionization of a BH type molecular orbital. In addition, bands corresponding to the ionization of orbitals associated mainly with the CO moieties¹⁴ and bands associated with ionization of filled orbitals of largely iron d character should appear (see Figure 1).

To verify these expectations and to begin the investigation of the $\text{Fe}(\text{CO})_3$ fragment in a cage environment, the molecules $\text{C}_2\text{B}_3\text{H}_5\text{Fe}(\text{CO})_3$ and $\text{C}_2\text{B}_3\text{H}_7\text{Fe}(\text{CO})_3$ were examined. The former has a bipyramidal (closo) arrangement of cluster atoms while the latter has a pyramidal (nido) geometry. The structure of the latter has been well defined by single-crystal x-ray diffraction studies¹⁶ and, recently, has been the subject of ab initio calculations.¹⁷

$\text{C}_2\text{B}_3\text{H}_5\text{Fe}(\text{CO})_3$. In this molecule the $\text{Fe}(\text{CO})_3$ fragment may be considered in either a ring or polar position. As the analogous compound, 1,6- $\text{C}_2\text{B}_4\text{H}_6$, was discussed with CH polar fragments, the $\text{Fe}(\text{CO})_3$ group will be considered to be in the ring fragment as indicated in Figure 2. The spectrum of $\text{C}_2\text{B}_3\text{H}_5\text{Fe}(\text{CO})_3$ is also displayed in Figure 2 with the numerical data being given in Table I. As detailed in the preceding paper, the primary experimental observations are band position, relative band intensity, relative band intensity as a function of photon energy, and fine structure. The key problem with the ferracarboranes and ferraboranes is the location of the orbitals involving the $\text{Fe}(\text{CO})_3$ group. Experimentally this is determined from band intensity as a function of photon energy. It has been demonstrated by earlier workers¹⁸ that for organometallics the relative intensity of bands associated with the iron atom and the carbonyl

Table I. Vertical Ionization Potentials, Relative Band Areas, and Band Assignments

Molecule	Band ^a	IP, ^b eV	A/E ^c (rel)	A/E (736 Å)/ A/E (584 Å)	IP per band	Assignment ^d
C ₂ B ₃ H ₅ Fe(CO) ₃	1	8.6	0.1	0.3	1	F
	2	9.1	0.2	0.6	2	F
	3	9.9	0.1	0.8	1	S, R
	4	11.2	0.3	0.9	2	S, RP
	5	11.9	0.4	1.1	2	Ex, R
	6	12.7	0.2	1.0	1	Ex, P
	7	14.7	1.4	0.6	10	F
C ₂ B ₃ H ₇ Fe(CO) ₃	1	13.8 sh 8.9 8.7 sh	0.3	0.7	3	F
	2	10.6	0.2	0.6	1	S, RP
	3	11.1	0.2	0.7	1	S, RP
	4	12.3	1.0	1.0	5	2Sp, 3Ex
	5	14.4	1.9	0.5	9+	F
B ₄ H ₈ Fe(CO) ₃	1	8.9 8.6 sh	0.4	0.7	3	F
	2	10.3	0.4	0.8	2	S, RP
	3	12.2	1.0	1.0	3	Ex, R, RP
	4	14.2	2.7	0.5	9+	F
C ₄ H ₄ Fe(CO) ₃	1	8.4 8.1 sh	0.4	0.7	3	F
	2	9.3	0.5	0.7	2	S, RP
	3	12.8	1.0	1.0	2	Ex, R
	4	13.9	2.6	0.7	9+	F
	5	17.3				
B ₅ H ₉ Fe(CO) ₃	1	8.4	0.1	0.6	1	S, RP
	2	9.2 8.9 sh	0.4	0.4	3	F
	3	10.8	0.2	0.9	1	S, RP
	4	11.5	0.4	1.0	5	2Sp, 3Ex
	5	12.4	1.0	1.0		
	6	14.4	2.2	0.5	9+	F
B ₅ H ₃ Fe(CO) ₅	1	8.0	0.1	0.6	1	F
	2	8.6	0.2	0.6	2	F
	3	9.2	0.2	0.7	1	S
	4	9.8	0.3	0.9	2	S
	5	10.7	0.4	1.2	2	Ex
	6	12.0	0.3	0.9	1	Ex
	7	14.0	1.8	0.7	9+	F
	8	16.6			2	CO (cage)

^a See figures for numbering. ^b Energies refer to band centers. sh refers to a shoulder on the band. ^c He(I) band area over mean electron energy. ^d F = Fe(CO)₃ fragment, S = surface orbital, Ex = exo-polyhedral orbital, R = ring orbital, RP = ring-polar interaction orbital, Sp = protonated surface orbital.

moieties of the Fe(CO)₃ fragment increase with increasing photon energy with respect to bands associated largely with main group atoms. These workers used the He(I) and He(II) lines whereas we use Ne(I) and He(I). For the case of metalboranes equivalent results are obtained with the latter sources and one has the added convenience of high photon intensity.¹⁹

It is quite evident in Figure 2 (also Table I) that the intensity of bands 1-2, 3, 4, and 7 decrease relative to the intensity of bands 5 and 6 in going from He(I) to Ne(I) radiation. The greatest change is seen in bands 1-2 and 7. The fact that these bands lie at about 8.5 and 14 eV, respectively, and that the ratio of the area of band 1-2 to band 7 is independent of photon energy (Table II) allows the assignment of band 1-2 to the ionization of the a and e orbitals associated with the iron (see Figure 1) and band 7 to the orbitals associated mainly with the CO's of the Fe(CO)₃ fragment. The assignment of these bands to the transferable orbitals of the Fe(CO)₃ fragment is unambiguous and is consistent with similar observations on organometallics containing the iron tricarbonyl fragment.¹⁸

The other bands are due to the ring, polar, and ring-polar interaction orbitals some of which will have iron character. The intensity data are not as clear-cut here because of the much smaller fraction iron character. However, what intensity change there is should be more evident in the π-endo orbitals than in the σ-exo (BH and CH) orbitals. If we assign bands 5 and 6 and the shoulder at low ionization potential on band 7 to the four highest lying σ-exo orbitals of the C₂B₄H₆ skeleton, then bands 3 and 4 must be due to the three π-endo orbitals.

Table II. Area Ratios of Bands Assigned to Fe(CO)₃ Transferable Fragment Orbitals

Compd	(A/E) _{Fe} /(A/E) _{CO}		Fe(a)/Fe(e) He(I)
	He(I)	Ne(I)	
C ₂ B ₃ H ₅ Fe(CO) ₃	0.18	0.15	0.65
C ₂ B ₃ H ₇ Fe(CO) ₃	0.15	0.20	
B ₄ H ₈ Fe(CO) ₃	0.15	0.23	
C ₄ H ₄ Fe(CO) ₃	0.16	0.17	
B ₅ H ₉ Fe(CO) ₃	0.17	0.14	
B ₅ H ₃ Fe(CO) ₅	0.15	0.13	0.72

The relative intensity data suggest that 3 and 4 have greater iron character than 5 and 6 but less than 1-2 and 7. In addition these data indicate that bands 4 and 5 result from the ionization of at least two orbitals. Exclusive of the bands to be associated with the Fe(CO)₃ fragment this assignment accounts for 7 of the 12 ionizations expected (3 π-endo, 5 σ-exo, and 4 σ-endo). With C₂B₄H₆ all four σ-endo orbitals and one σ-exo orbital lie above 17 eV; thus the indicated assignment is reasonable. Naturally, one cannot exclude the possibility that one or two of the five other expected bands are lost in the large "CO" band at 14 eV.

A schematic representation of this assignment is given at the bottom of Figure 2. Quantitatively comparing this assignment with the

analysis of 1,6- $C_2B_4H_6$ one finds that for the ring orbitals α has shifted from -12.4 to -11.9 eV and β from -1.3 to -1.0 eV.⁶ Both changes are reasonable in view of the lower electronegativity of Fe with respect to boron and in terms of less mixing due to the larger Fe atom. The ring-polar interaction orbitals are both shifted down by about 1 eV which is also reasonable in terms of relative electronegativities, smaller ring-polar interactions or both. Thus, when the additional features introduced by the $Fe(CO)_3$ fragment into the photoelectron spectrum are taken into account, an adequate explanation of the observed features of the spectrum of $C_2B_3H_5Fe(CO)_3$ results by simply treating the $Fe(CO)_3$ fragment as BH and applying the ring-polar model.

Recently, it has been suggested that the reason why the analogy between the structures of boranes and transition metal clusters works is that species like $B_6H_6^{2-}$ and $Co_6(CO)_{14}^{4-}$ have similar s and p overlap integrals.^{10,20} The photoelectron spectra of $C_2B_3H_5Fe(CO)_3$ suggest that the analogy is basically correct for mixed clusters as well.

$C_2B_3H_7Fe(CO)_3$. This molecule provides a test of the BH- $Fe(CO)_3$ substitution technique for the pyramidal case. The structure of $C_2B_3H_7Fe(CO)_3$ according to the x-ray diffraction results¹⁶ is shown in Figure 3. The $Fe(CO)_3$ group is in a polar position while the analogous carborane, 2,3- $C_2B_4H_8$, has a BH group in the corresponding polar (apical) position. The spectra of $C_2B_3H_7Fe(CO)_3$ are given in Figure 3 and are tabulated in Table I. Band positions, relative intensities (see also Table II), and intensity as a function of photon energy show that bands 1 and 5 are due to the transferable filled orbitals of the iron tricarbonyl fragment. Using 2,3- $C_2B_4H_8$ as a guide, we would expect seven additional ionizations between 9 and 14 eV. If bands 2 and 3 result from the ionization of single orbitals, the relative areas suggest that band 4 results from the ionization of four to six orbitals. Intensity vs. photon energy (Table I) suggests that 2 and 3 are π -endo orbitals with significant iron content leading to the assignment schematically illustrated in Figure 3. Bands 2 and 3 are assigned to ring-polar interaction orbitals involving the apical iron. It is suggested that band 4 contains five ionizations: one ring-polar interaction and four ring orbitals.

Once the bands associated strictly with the $Fe(CO)_3$ group are accounted for the remainder of the spectrum can be adequately explained on the basis of the analogous carborane. In this case, however, the lower symmetry yields a less structured spectrum and the fit is somewhat less convincing than in the case of $C_2B_3H_5Fe(CO)_3$. In addition there appears to be one significant difference between the ferracarborane and the carborane. In the latter the splitting between the ring-polar interaction orbitals, which was attributed to an unsymmetrical placement of the carbon atoms and bridging protons with respect to the p_x and p_y orbitals of the apical atom, is 1.7 eV⁶ while in the above assignment for the ferraborane it is 0.5 eV. This would suggest that the splitting of the ring-polar interaction orbitals is not as sensitive to substitution of heteroatoms in the boron ring or ring protonation when $Fe(CO)_3$ is the polar fragment. A possible explanation is a weaker interaction of the metal orbitals with the ring compared to either BH or CH. This is consistent with the lower mixing of the iron orbitals with the main group orbitals found in $C_2B_3H_5Fe(CO)_3$.

The orbital energies from SCF calculations¹⁷ are included in Figure 3 by utilizing Koopmans' theorem. There is agreement between the model predictions and the calculations concerning the number of orbitals in the region below 13 eV. (This corresponds to roughly 15 eV down for the calculations.) Beyond this there is little correlation between the empirical assignment and the calculations. In one sense this is not surprising as similar type calculations for organometallics have demonstrated much greater Koopmans' defects for the metal orbitals in a compound than for orbitals constructed of main group atomic orbitals.¹⁸ There is, however, a difference that cannot be accounted for by inadequacies in Koopmans' theorem. In the calculations, the four orbitals indicated in Figure 3 with the letter M have large metal character. The photoelectron spectra indicate that bands 1, 2, and 3 have high metal character and, according to the empirical assignment, result from the ionization of 5 orbitals. Thus, either band 1 contains only two ionizations or the calculations do not properly reflect the mixing of the metal and ring orbitals. If the former is true then $C_2B_3H_7Fe(CO)_3$ is different from other molecules containing the $Fe(CO)_3$ fragment. If the latter is true then the main argument for largely ionic bonding between the ring and the $Fe(CO)_3$ fragment collapses. The data in Tables II and III suggests that the $Fe(CO)_3$ fragment behaves consistently in all the compounds studied including

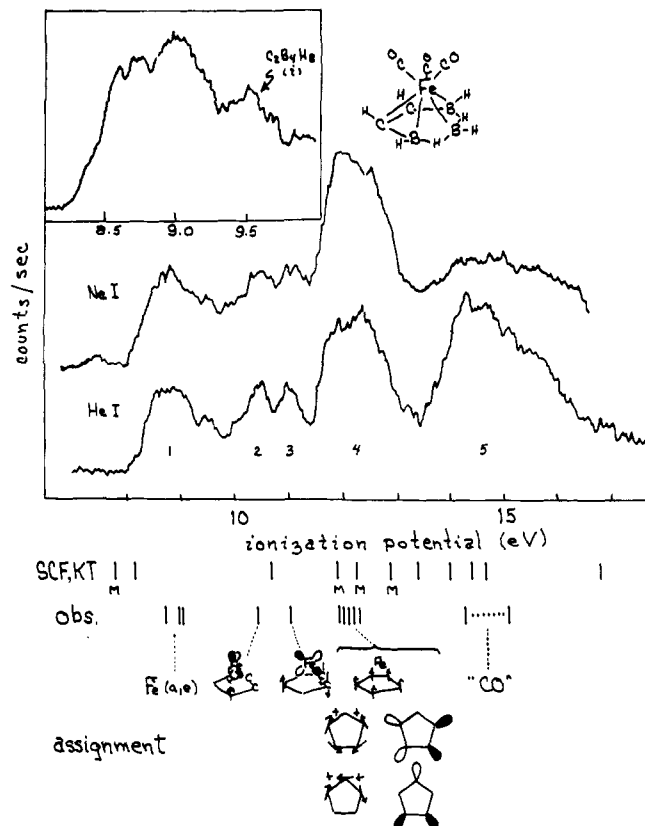


Figure 3. The photoelectron spectra of $C_2B_3H_7Fe(CO)_3$ and the orbital assignments. The inset shows the first bands with expanded scale and He(I) photon source. The spectra contain a small amount of $C_2B_4H_8$ as an impurity. The SCF orbital energies are from Figure 2 of ref 17. The letter "M" indicates large metal character.

one that has a bridging hydrogen to the iron atom. Thus, we feel justified in concluding that for the purposes of assigning the photoelectron spectra of metal compounds, the empirical method is superior to ground-state only calculations.

The Ferraboranes. $B_4H_8Fe(CO)_3$. This molecule consists of a B_4H_8 ring with a polar $Fe(CO)_3$ fragment¹ as indicated by the structure at the top of Figure 4. Thus, it is a metallo analogue of B_5H_9 . The He(I) and Ne(I) spectra of $B_4H_8Fe(CO)_3$ are given in Figure 4 and the data are gathered in Table I. Once again the He(I)/Ne(I) relative intensity data, band energies, and area ratios (Table II) identify bands 1 and 4 as being due to orbitals situated mainly on the $Fe(CO)_3$ fragment. In addition the data suggest that band 2 has significant Fe character. The relative intensities of bands 2 and 3 suggest that the number of orbitals ionized are in the ratio of 2 to 3. Using the parameters developed for the B_4H_8 ring and treating the $Fe(CO)_3$ ring interaction as a BH-ring interaction yields the assignment indicated at the bottom of Figure 4. In this assignment band 2 results from ionization of the doubly degenerate π -endo orbital involving Fe and the ring. Again the most striking observation is that once the characteristic transferable bands due to the $Fe(CO)_3$ fragment are removed, the remaining bands are almost identical with the corresponding borane.⁶ The only difference is a small shift of the bands to lower ionization potential.

$C_4H_4Fe(CO)_3$. As noted previously, $B_4H_8Fe(CO)_3$ can also be considered an analogue of $C_4H_4Fe(CO)_3$. The spectra of the latter compound are given in Figure 5 along with Koopmans's theorem SCF results.¹⁸ The assignment of the bands according to the empirical model being employed here is indicated at the bottom of the figure. The assignment gives essentially the same orbital compositions as those derived previously.¹⁸ However, a couple of comments are in order. Previous workers used He(I)/He(II) intensity data to distinguish the "CO" and Fe(a,e) orbitals. Here the He(I)/Ne(I) intensity data reveal the "CO" band but in contrast to the He(I)/He(II) data do not reveal any difference in the metal character of bands 1 and 2. This is not unreasonable as the cross section for carbon 2p does not rise as rapidly as boron 2p in going from 21.2 to 16.8 eV.²¹ Thus, the He(I)/Ne(I)

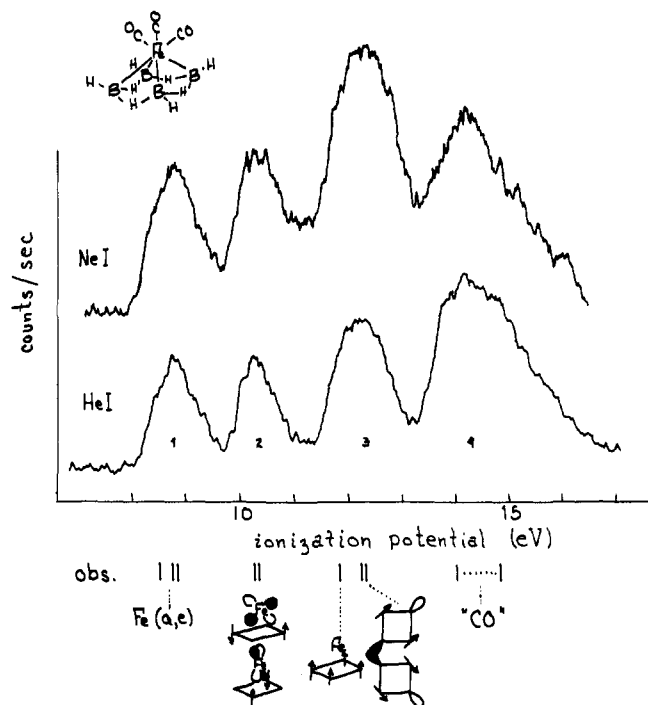
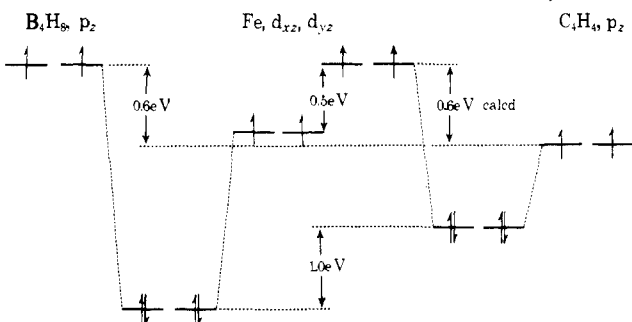


Figure 4. The photoelectron spectra of $B_4H_8Fe(CO)_3$ and the orbital assignments.

experiment is not as sensitive as He(I)/He(II) and will not be as useful in organometallic systems. In this particular case the shoulder on band 1 strongly suggests that it is due to ionization of the Fe(a,e) orbitals. Note that the problem of a large apparent²² Koopmans' defect for metal orbitals which continues to generate much discussion and some controversy,²³ is by-passed with the empirical model employed here. If these defects are real then our individual orbital assignments apply only to the ion. However, as our primary interest is in probing changes in chemical properties in series of related molecules the problem of Koopmans' theorem breakdown is not of crucial interest.²⁴

Having assigned the spectra, corresponding bands for $C_4H_4Fe(CO)_3$ and $B_4H_8Fe(CO)_3$ may be compared. In both compounds band 3 results from orbitals associated mainly with the main group ring. As expected on the basis of nuclear charge this band shifts to slightly higher energy (lower ionization potential) as one goes from C_4H_4 to B_4H_8 . Band 1 is assigned to ionization of the Fe(a,e) orbitals and, somewhat surprisingly, it shifts to higher ionization potential as one goes from C_4H_4 to B_4H_8 . Apparently, in the organometallic compound the iron atom is better able to accommodate the positive hole. This may be due to more electron density on the iron or greater stabilization of the hole in the ion in the case of $C_4H_4Fe(CO)_3$. Band 2 is assigned to ionization of the pair of ring-polar interaction (π -endo type) orbitals in both compounds. As indicated in the energy level diagram below, these orbitals originate from the Fe d_{xz} and d_{yz} orbitals



and the corresponding symmetry combinations of ring p_{yz} orbitals and the corresponding symmetry combinations of ring p_z orbitals. The energy difference of the metal orbitals may be estimated from the Fe(a,e) bands in the two compounds and the energy difference in the filled orbitals from the positions of band 3 in the two compounds, i.e., 0.6 eV.

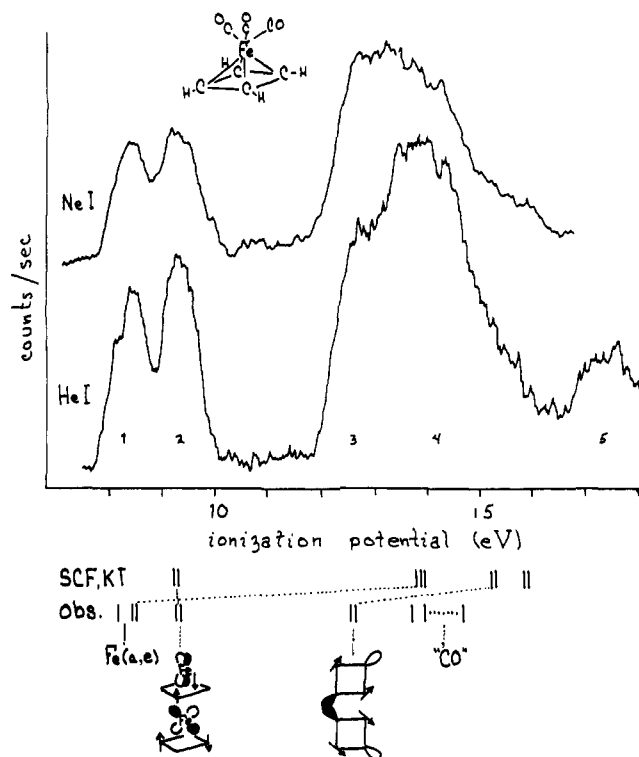


Figure 5. The photoelectron spectra of $C_4H_4Fe(CO)_3$ and the orbital assignments.

The relative energy of the cyclobutadiene ring orbitals with respect to the metal orbitals is taken from the extended Hückel results.¹³ All this suggests that the lower energy of the metal-ring orbital in the ferraborane results from a larger interaction between the metal and borane ring compared to the metal and carbon ring. Thus, the iron appears more cage-like in $B_4H_8Fe(CO)_3$ than in $C_4H_4Fe(CO)_3$. This may be compared to the observation above that $Fe(CO)_3$ appears less cage-like in $C_2B_3H_7Fe(CO)_3$ than BH in $C_2B_4H_8$.

$B_5H_9Fe(CO)_3$. This species is formed along with $B_4H_8Fe(CO)_3$ in the copolyrlysis of B_5H_9 and $Fe(CO)_5$.² The physical data and a single-crystal x-ray diffraction study of the anion $B_5H_8Fe(CO)_3^-$ show that the molecule has the structure indicated in Figure 6, i.e., a pentagonal pyramidal arrangement of the iron atom and borons with the $Fe(CO)_3$ fragment being in the basal plane.² As such its structure formally represents that of B_6H_{10} ; however, there is a very interesting difference associated with the bridging hydrogen attached to both boron and iron. Both the location and spin coupling to ^{11}B suggest a B-H-Fe bridge. On the other hand, the Fe-H distance, although approximate, is more consistent with a terminal H. In addition the fluxional behavior of this hydrogen suggests B-H breaking rather than H-M breaking as observed in other hydrogen metal bridged systems. As it has been demonstrated that the splitting of the two highest lying π -endo orbitals (ring-polar interaction orbitals) depends strongly on the ring composition and the number of bridging hydrogens, the electronic structure of $B_5H_9Fe(CO)_3$, i.e., the photoelectron spectrum, should reflect the role of the B-H-Fe hydrogen.

The He(I) and Ne(I) spectra of $B_5H_9Fe(CO)_3$ are given in Figure 6 and the vertical ionization potentials and relative area data appear in Table I. Clearly band 6 is associated with the CO's of the $Fe(CO)_3$ fragment and bands 1 and 2 have significant iron character. The crucial assignment here is band 1 and 2. In this region we expect the Fe(a,e) ionizations and one or two ring-polar interaction orbitals depending on whether the electronic structure is more similar to $B_6H_{10}/C_2B_4H_8$ or CB_5H_9 . Previously, on the basis of data taken at a single photon energy, we assigned the strong peak of band 2 to ring-polar interactions and band 1 plus the shoulder of band 2 to Fe(a,e).² Thus, the CB_5H_9 molecule was taken to be a good model for $B_5H_9Fe(CO)_3$, i.e., the B-H-Fe hydrogen was to be associated more with the iron than the cage. However, the Ne(I) results (upper spectrum, Figure 6) demonstrate that this assignment is incorrect. Band 2 loses more intensity than band 1 in going to the lower photon energy

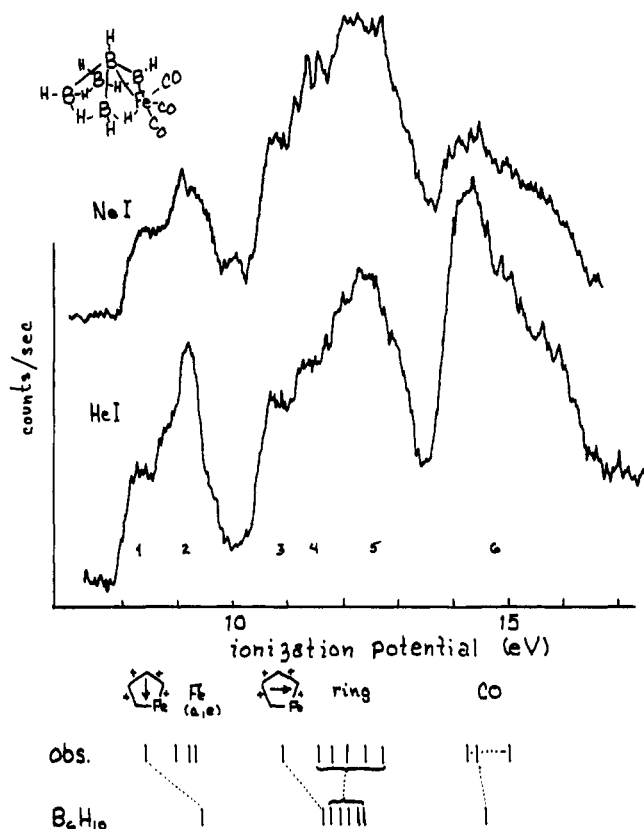


Figure 6. The photoelectron spectra of $B_5H_9Fe(CO)_3$ and the orbital assignments.

(Table I). Therefore, band 2 must be assigned to Fe(a,e) ionization. The area of this band relative to the "CO" band is consistent with that for the other compounds (Table II). The small relative area of band 1 strongly suggests that it results from the ionization of a single orbital. Consequently, bands 3, 4, and 5 are assigned to the ionization of the other six orbitals expected. The area measurements on bands 3, 4, and 5 are consistent with this assignment. Of the six orbitals in bands 3, 4, and 5, four or five should have little iron character. This is substantiated by the He(I)/Ne(I) intensity changes. Band 1 does show some iron character and the band is attributed to ionization of a ring-polar orbital (π -endo) as indicated at the bottom of the figure. Note that with BH in the apical position the splitting between the two surface orbitals (bands 1 and 3) is about the same as that in B_6H_{10} . It seems then that B_6H_{10} (or $C_2B_4H_8$) is a better model for the electronic structure of this ferraborane than CB_5H_9 . Of all the ferraboranes studied, this is the only one that has a framework band lying at lower ionization potential than the metal d bands. As all Koopmans' defects observed would tend to further separate the corresponding orbitals in the molecule, this constitutes a clear example of a ferraborane with a highest occupied molecular orbital of framework character. Thus, insofar as the HOMO is related to reactivity this compound should behave like B_6H_{10} . Indeed Shore and co-workers have demonstrated many similarities between the chemistry of the two compounds.²⁵

$B_5H_3Fe(CO)_5$. Another unusual ferraborane has been isolated from the products of the pyrolysis of B_3H_9 with $Fe(CO)_5$.³ On the basis of physical data, the compound is identified as $B_5H_3Fe(CO)_5$ and the postulated structural consistent with the structural data is shown at the top of Figure 7. The unique feature of this molecule, which is an analogue of the $B_6H_6^{2-}$ ion, is that it possesses both an $Fe(CO)_3$ group and two CO's bound to the borane cage. Cage bound carbonyls are known in larger borane cages²⁶ but this is the first example of a metallaborane with such a feature. Consequently, the characterization of the molecule is of intense interest particularly in regard to the mode of bonding of the carbonyl to the cage.

The He(I) and Ne(I) spectra of $B_5H_3Fe(CO)_5$ are given in Figure 7 and the data are summarized in Table I. The He(I)/Ne(I) relative intensity data clearly indicate that bands 1, 2, and 3 are associated strongly with iron, band 7 is due to the CO's of the $Fe(CO)_3$ fragment,

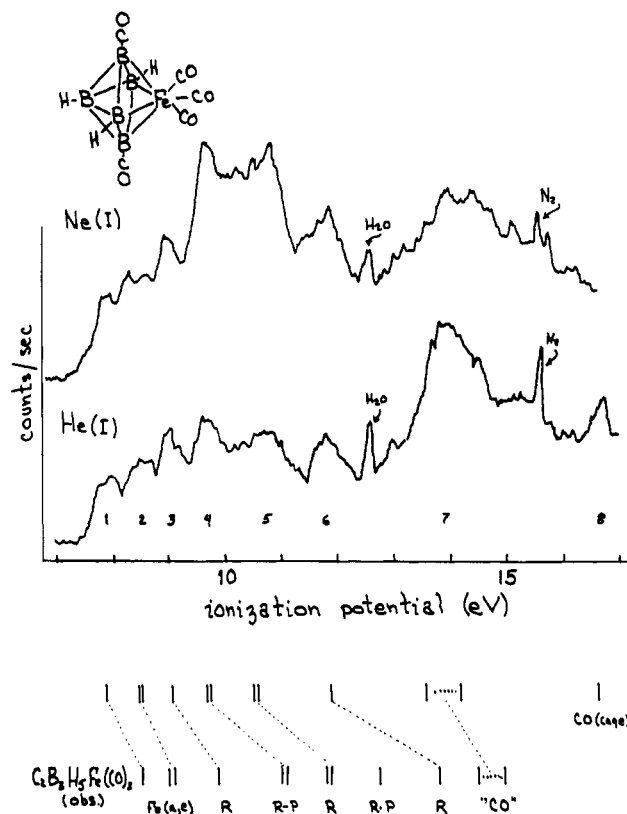


Figure 7. The photoelectron spectra of $B_5H_3Fe(CO)_5$ and the orbital assignments. "R" represents ring orbital, "R-P" represents ring-polar interaction orbital, and "CO (cage)" represents the former 1π orbitals of the CO bound to the cage.

and bands 4, 5, and 6 are associated with the boron framework. For the purposes of this discussion only the structure with 1,6 CO's (Figure 7) will be considered although the existing structural data cannot rule out the 1,2 isomer. The appropriate model compound here is $C_2B_3H_5Fe(CO)_3$ and the observed energy level diagram for this species (see also Figure 2) is given at the bottom of Figure 7.

First, we expect to see bands due to ionization of the Fe(a,e) and iron "CO" orbitals and bands 1, 2, and 7 are so assigned. Note that the ratio of the Fe(a,e) band area to that of the "CO" band area is the same in this compound as in all the other compounds containing the $Fe(CO)_3$ fragment. This is additional confirmation that there is indeed an $Fe(CO)_3$ fragment in the molecule.

Second, in the ring-polar model both $C_2B_3H_5Fe(CO)_3$ and $B_5H_3Fe(CO)_5$ should have the same set of four ring orbitals centered between 10 and 12 eV. Of these four the one at lowest ionization potential should have significant iron character. Bands 5, and 6 have the required characteristics and are assigned to the $B_3H_3Fe(CO)_3$ ring.

Third, the two bands associated with the exo CH orbitals in $C_2B_3H_5Fe(CO)_3$ at 12.7 and about 17 eV are lost and replaced by the bands associated with the cage CO's. Each CO will introduce three orbitals in the energy range under consideration, i.e., one corresponds to the former 5σ orbital and two to the 1π . A reasonable model for locating the approximate position of the bands is BH_3CO , the adduct of BH_3 and CO, which has been extensively studied. Of pertinence here are the results of a photoelectron spectroscopic study²⁷ in which it was shown that the orbitals in BH_3CO correlating with the 5σ and 1π shift very little on coordination to boron. The coordinated 5σ was assigned to a band at 14.1 eV and the 1π to a band at 17.0 eV. It will be noted that there is a band in the He(I) spectrum of $B_5H_3Fe(CO)_5$ at 16.6 eV that is not present in the model compound. We suggest that this band corresponds to the ionization of the cage coordinated CO 1π orbitals. If so, the 5σ ionizations would be found under the $Fe(CO)_3$ "CO" band at 14 eV. The two additional ionizations thus added to the band are well within the error of area measurements.

One reason presented for the small shift between coordinated CO and uncoordinated CO in BH_3CO is the presence of back-donation to the CO π^* orbitals. Such an effect is certainly possible with clusters

Table III. Splitting of "a" and "e" Fe Orbitals as a Function of Cage Geometry

Compd	Structure ^a	Position Fe	Splitting, eV	Band center of gravity, eV
B ₄ H ₈ Fe(CO) ₃	py	Apex	0.31	8.90
C ₄ H ₄ Fe(CO) ₃	py	Apex	0.28	8.39
B ₅ H ₉ Fe(CO) ₃	py	Base	0.37	9.26
C ₂ B ₃ H ₇ Fe(CO) ₃	py	Apex	0.32	8.92
B ₅ H ₃ Fe(CO) ₅	bipy		0.56	8.21
C ₂ B ₃ H ₅ Fe(CO) ₃	bipy		0.50	8.66

^a py ≡ pyramid, bipy ≡ bipyramid.

as well, as the π -endo orbitals of the cluster have the proper symmetry to interact with the π^* orbitals of the CO. Evidence that such π type interactions with π -endo orbitals do take place has resulted from a study of the perturbation of π -endo orbitals by filled π -type orbitals of exo substituents on both nido²⁸ and closo²⁹ cages.

By itself this analysis of the observed spectrum of B₅H₃Fe(CO)₅ does not prove the structure. On the other hand, all the features one expects on the basis of the postulated structure do appear in the observed spectrum. The only major difference between the spectrum of the model compound and that of B₅H₃Fe(CO)₅ is a general shift of bands to lower ionization potential which may well be due to the effect of replacing two carbons with two borons. The data do not distinguish between the 1,6 and 1,2 isomers although it is tempting to say that the general correspondence of C₂B₃H₅Fe(CO)₃ with B₅H₃Fe(CO)₅ favors the former arrangement of cage CO's.

Conclusions

In proceeding beyond the simple assignment and rationalization of the observed spectra, consider first the conclusions concerning the Fe(CO)₃ as affected by the borane or carborane fragment. Any transferable orbital of this fragment is a usable probe of charge effects; however, the Fe(a,e) orbitals are the best choice. The ionization potential of the corresponding band is the energy necessary to create a hole at the iron center. Both the properties of the ion and molecule govern the magnitude of this energy. Factors usually discussed are the charge on the iron atom in the molecule, charge relaxation in the ion, and loss of correlation energy on ionization. Despite the complex nature of the ionization energy it may be used to see how the ability of the iron atom to accommodate a positive charge changes with the nature of the borane skeleton. The numbers of interest are gathered in Table III. For all except one borane fragment the average ionization energy of these iron orbitals is higher than in C₄H₄Fe(CO)₃, i.e., it is more difficult to remove charge from the iron when the organic ligand is replaced by a borane or carborane ligand. The one exception is B₅H₃Fe(CO)₅, which has carbonyls bound to the cage itself. An explanation in terms of charge distribution in the molecule alone is that the "electron-deficient" frameworks effectively remove more electron density from the iron than the organic moiety. In the case of B₅H₃Fe(CO)₅, the cage bound CO's must reduce the effective electronegativity of the cage. It is curious to note that the ionization energy for B₅H₃Fe(CO)₃ is the highest value. This is the only compound with a B-H-Fe bridge and it is quite reasonable that the presence of the proton in the vicinity of the iron results in an increased effective potential at the iron. Note that in H₂Fe(CO)₄ the iron d bands appear at an energy of 9.65 eV.³⁰

The second point to notice in the data in Table III is that the splitting between the orbitals assigned to Fe(a) and Fe(e) depends on the structure of the entire cluster, the splitting being larger for bipyramidal (closo) than for pyramidal (nido) structures. Although the numbers are not very precise, there is a qualitative difference between the two sets. It has been demonstrated in calculations¹³ that the splitting between these

orbitals is a function of the angle θ between the threefold symmetry axis and the Fe-C-O bond (see Figure 1). In addition the composition of the Fe(e) orbitals varies with this angle going from xz and yz at 130° to xy and $x^2 - y^2$ at 90°.¹³ We suggest that the pyramidal and bipyramidal situations place different requirements on the iron atom, thereby resulting in different θ 's and different Fe(a,e) splittings. Whether or not this explanation is correct, it appears that the empirical splitting can be used to distinguish the Fe(CO)₃ fragment in different environments.

Alternatively, attention may be focused on the cage in terms of how it is affected by the Fe(CO)₃ fragment. First it is emphasized again that the equivalence of Fe(CO)₃ and BH in a cage is more than a rule of thumb. At least from the standpoint of photoelectron spectroscopy, the electronic structure of the cage is qualitatively unaffected by the substitution. In quantitative terms it appears that with the possible exception of C₂B₃H₇Fe(CO)₃ the substitution of Fe(CO)₃ for BH results in a small shift in the ionization energies of equivalent bands to lower values. Placement of the metal in the cage appears to lower the effective potential seen by the cage orbitals. The iron has one other effect on the electronic structure of the cage that might be forgotten in the effort to identify a ferraborane with an equivalent borane. Not only does the iron introduce additional filled orbitals, e.g., Fe(a,e), but it will also increase the number of unfilled orbitals. Thus, more structural variation is expected with metals than with main group atoms.^{9,31}

The empirical model developed in the previous paper and used here does provide useful information. The information is not as detailed as one might like as one is limited by preparative problems; however, in every case the highest occupied molecular orbitals have been qualitatively depicted in terms of atomic orbital composition and energy. It will be worthwhile to extend this approach to cages containing more than a single metal atom and work on multimetal clusters is in progress.

Acknowledgments. The support of the National Science Foundation through Grant CHE75-10938 A01 and the support of the donors of the Petroleum Research Fund, administered by the American Chemical Society, are gratefully acknowledged.

References and Notes

- (1) N. N. Greenwood, C. G. Savory, R. N. Grimes, L. G. Sneddon, A. Davison, and S. S. Wreford, *J. Chem. Soc., Chem. Commun.*, 718 (1974).
- (2) T. P. Fehlner, J. Ragaini, M. Mangion, and S. G. Shore, *J. Am. Chem. Soc.*, **98**, 7085 (1976).
- (3) J. A. Ulman and T. P. Fehlner, *J. Chem. Soc., Chem. Commun.*, 632 (1976).
- (4) D. W. Turner, C. Baker, A. D. Baker, and C. R. Brundle, "Molecular Photoelectron Spectroscopy", Wiley-Interscience, New York, N.Y., 1970.
- (5) See, for example, M. Rohmer and A. Viellard, *J. Chem. Soc., Chem. Commun.*, 250 (1973).
- (6) J. A. Ulman and T. P. Fehlner, *J. Am. Chem. Soc.*, preceding paper in this issue.
- (7) E. L. Muetterties, "Boron Hydride Chemistry", Academic Press, New York, N.Y., 1975.
- (8) M. F. Hawthorne, *J. Organomet. Chem.*, **100**, 97 (1975).
- (9) K. Wade, *Adv. Inorg. Chem. Radiochem.*, **18**, 1 (1976); R. E. Williams, *ibid.*, **18**, 67 (1976); R. W. Rudolph, *Acc. Chem. Res.*, **9**, 446 (1976).
- (10) D. M. P. Mingos, *J. Chem. Soc., Dalton Trans.*, 602, 610 (1977).
- (11) V. R. Miller, L. G. Sneddon, D. C. Beer, and R. N. Grimes, *J. Am. Chem. Soc.*, **96**, 3090 (1974).
- (12) R. N. Grimes, *J. Am. Chem. Soc.*, **93**, 261 (1971).
- (13) M. Eilan and R. Hoffmann, *Inorg. Chem.*, **14**, 1058 (1975).
- (14) Three orbitals per CO are expected in the 13.5–15.5-eV region.
- (15) This conclusion is supported by the recorded spectra of other organometallics containing the Fe(CO)₃ fragment. See, for example, J. A. Connor, L. M. R. Derrick, M. B. Hall, I. H. Hillier, M. F. Guest, B. R. Higginson, and D. R. Lloyd, *Mol. Phys.*, **28**, 1193 (1974).
- (16) J. P. Brennan, R. N. Grimes, R. Schaeffer, and L. G. Sneddon, *Inorg. Chem.*, **12**, 2266 (1973).
- (17) D. R. Armstrong and R. H. Findlay, *Inorg. Chim. Acta*, **21**, 55 (1977).
- (18) M. B. Hall, I. H. Hillier, J. A. Connor, M. F. Guest, and D. R. Lloyd, *Mol. Phys.*, **30**, 839 (1975).
- (19) The two approaches are directly compared with C₄H₄Fe(CO)₃ below.
- (20) D. M. P. Mingos, *J. Chem. Soc., Dalton Trans.*, 133 (1974).
- (21) J. W. Rabalais, "Principles of Ultraviolet Photoelectron Spectroscopy", Wiley, New York, N.Y., 1977, p 335.

- (22) "Apparent" is used because it is not clear that this is not just another basis set problem.
- (23) C. D. Batich, *J. Am. Chem. Soc.*, **98**, 7585 (1976).
- (24) The results of calculations on ferrocene and ferricinium suggest that substantial charge redistribution does occur upon ionization: P. S. Bagus, U. I. Walgren, and J. Almlof, *J. Chem. Phys.*, **64**, 2324 (1976).
- (25) J. Ragaini, M. M. Mangion, and S. G. Shore, Abstracts, 172nd Meeting of the American Chemical Society, San Francisco, Calif., Aug-Sept 1976, No. INOR-85.
- (26) W. H. Knoth, *J. Am. Chem. Soc.*, **88**, 935 (1966).
- (27) D. R. Lloyd and N. Lynaugh, *J. Chem. Soc., Faraday Trans. 2*, **68**, 947 (1972).
- (28) J. A. Ulman and T. P. Fehlner, *J. Am. Chem. Soc.*, **98**, 1119 (1976).
- (29) G. Beltram and T. P. Fehlner, in preparation.
- (30) M. F. Guest, B. R. Higginson, D. R. Lloyd, and I. H. Hillier, *J. Chem. Soc., Faraday Trans. 2*, **71**, 902 (1975).
- (31) See ref 10 for a discussion of metallocarborane cages for which the predictions based on electron counting are not correct in detail.

The Solution Photosubstitution Chemistry of Triphenylphosphine Derivatives of Molybdenum Hexacarbonyl

Donald J. Darensbourg* and Mark A. Murphy

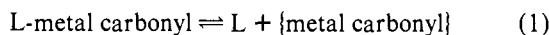
Contribution from the Department of Chemistry, Tulane University, New Orleans, Louisiana 70118. Received July 15, 1977

Abstract: The ligand photosubstitution chemistry of $\text{Mo}(\text{CO})_5\text{PPh}_3$ has been demonstrated to proceed with a high quantum efficiency for CO loss ($\Phi_{366} = 0.58$). When this reaction was carried out in the presence of either PPh_3 or ^{13}CO both *cis* and *trans* primary photoproducts were observed, presumably resulting from incoming ligand trapping of the $[\text{Mo}(\text{CO})_4\text{PPh}_3]$ intermediate in its C_s or C_{4v} isomeric forms, respectively. On the other hand, the quantum efficiency for unique ligand loss, PPh_3 , was only 0.11 at 366 nm. The *trans*- $\text{Mo}(\text{CO})_4[\text{PPh}_3]_2$ complex was found to undergo photoisomerization to the *cis*- $\text{Mo}(\text{CO})_4[\text{PPh}_3]_2$ derivative via loss of PPh_3 followed by subsequent rearrangement of the $[\text{Mo}(\text{CO})_4\text{PPh}_3]$ (C_{4v}) intermediate to its C_s analogue prior to recapture of PPh_3 . Photolysis of either pure *cis*- or *trans*- $\text{Mo}(\text{CO})_4[\text{PPh}_3]_2$ in the presence of ^{13}CO afforded primarily *cis*- $\text{Mo}(\text{CO})_4(^{13}\text{CO})\text{PPh}_3$ with a smaller quantity of *trans*- $\text{Mo}(\text{CO})_4(^{13}\text{CO})\text{PPh}_3$. The latter ^{13}CO -labeled species was observed in larger quantities from photolysis of *trans*- $\text{Mo}(\text{CO})_4[\text{PPh}_3]_2$ with ^{13}CO as would be anticipated. These experiments further demonstrate the facile rearrangement of the C_{4v} structure of $[\text{Mo}(\text{CO})_4\text{PPh}_3]$ to the C_s structure prior to recombination with an incoming ligand.

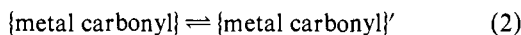
Introduction

Ligand substitution is probably the most important photochemical reaction of metal carbonyl derivatives.¹⁻⁵ This is primarily due to the fact that photosubstitution chemistry is an essential aspect of photoinitiated transition metal carbonyl catalysis. The three steps in the photo- or thermal-substitution processes are illustrated below:

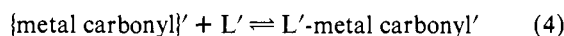
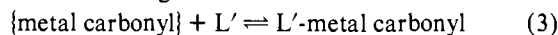
Ligand dissociation



Intermediate transformation

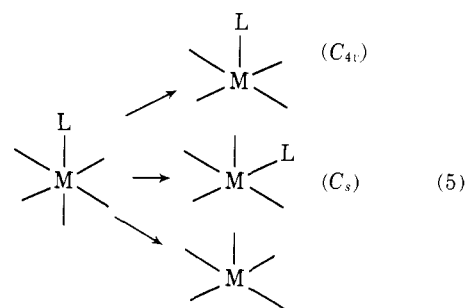


Ligand combination



As indicated in eq 1, during the photochemical process coordinatively unsaturated species can be produced under rather mild conditions. The nature of these intermediates and the stereochemical position of the ligand dissociated is a point of much interest since this information leads to an understanding of the structure and reactivity of these coordinatively unsaturated species which are ubiquitous in homogeneous catalysis. It is important to note that these intermediates can exhibit isomerization in photoexcited states. For example, Poliakoff has shown that the five-coordinate intermediate resulting from CO loss in matrix-isolated *trans*- $(^{13}\text{CO})\text{-W}(\text{CO})_4\text{CS}$, $[(^{13}\text{CO})\text{W}(\text{CO})_3\text{CS}]$, undergoes rearrangement in an electronic or vibrational excited state.⁶ Black and Bra-

terman have also reported that the axial square-pyramidal isomer of $[\text{Mo}(\text{CO})_4\text{P}(\text{C}_6\text{H}_{11})_3]$ generated by photolysis of $\text{Mo}(\text{CO})_5\text{P}(\text{C}_6\text{H}_{11})_3$ in a hydrocarbon matrix isomerizes to the equatorial isomer via a photochemical process.⁷ In addition it is also apparent that thermal rearrangements of unsaturated transition metal carbonyls often occur.⁸⁻¹⁰



Upon photolysis of $\text{M}(\text{CO})_5\text{L}$ species under conditions of ligand substitution, three reaction pathways are available (eq 5). When photoejection of carbon monoxide occurs, the loss of an axial CO group affords the C_{4v} isomer, whereas the loss of an equatorial CO group leads to the C_s isomer.

We have previously shown via stereospecific ^{13}CO labeling that the $[\text{Mo}(\text{CO})_5]$ intermediate afforded thermally from $\text{Mo}(\text{CO})_5\text{NHC}_5\text{H}_{10}$ in solution readily rearranges CO ligands, presumably through the square-pyramidal equivalent of the Berry pseudorotation ($C_{4v} \rightarrow D_{3h} \rightarrow C_{4v}$).¹¹ Similar observations have also been made in the matrix photochemistry of group 6B hexacarbonyl species.¹² In cases where one of the isomeric forms of $[\text{M}(\text{CO})_4\text{L}]$ (C_s or C_{4v}) is produced pref-